STATIC BENDING ANALYSIS OF VARIABLE THICKNESS MICROPLATES USING THE FINITE ELEMENT METHOD AND MODIFIED COUPLE STRESS THEORY

Thi Cam Nhung Nguyen[1,*], Minh Hoang Le[1], Van Ke Tran[1], Thi Dung Nguyen[1], Van Minh Phung[1]

[1]*Faculty of Mechanical Engineering, Le Quy Don Technical University, Hanoi, Vietnam*

Abstract

This paper presents the nonlinear static bending analysis of variable thickness microplates by using the finite element method and modified couple stress. The present theory and mathematical model are confirmed by comparing the numerical data with those of open literatures. A parameter study is carried out to investigate the mechanical behavior of the structure, especially, the effect of nonlinearlity. The computed data can be used as a good reference in the use and design of these types of structures in engineering practice.

Keywords: *Nonlinear; microplate; modified couple stress; static bending; variable thickness.*

1. Introduction

Nowadays, with the great development of materials technology, materials with micro and nano size have been studied and widely used in modern industries [1-4]. Therefore, the study of the mechanical behavior of these structures plays an extremely important role. The theories that calculate beams, plates and shells for traditional structures are no longer suitable to accurately describe the mechanical behavior relationships of micro and nanostructures. Therefore, many different theories have been developed to study the mechanical response of micro and nano structures. Along with that, the research achievements on this structure have also achieved many rich results [5-9].

In fact, the structure often undergoes large deformation, so the views about the linear relationship between the mechanical components will sometimes be incorrect. Therefore, calculating the nonlinear mechanical behavior of the structure is very important. Chen et al. [10] investigated size-dependent nonlinear bending behavior of porous FGM quasi-3D microplates with a central cutout based on nonlocal strain gradient isogeometric finite element modelling. Nonlinear analysis of size-dependent annular sector and rectangular microplates under transverse loading and resting on foundations based on the modified couple stress theory was carried out by Alinaghizadeh and Shariati [11]. Ghayesh and colleages [12] studied nonlinear

[*] Email: camnhungktqs@gmail.com

oscillations of functionally graded microplates. Askari and Tahani [13] introduced size-dependent dynamic pull-in analysis of geometric non-linear micro-plates based on the modified couple stress theory. Şimşek et al. [14] explored size-dependent vibration of a microplate under the action of a moving load based on the modified couple stress theory. Farokhi and his co-workers [15] investigated nonlinear oscillations of viscoelastic microplates. Thai and Choi [16] presented size-dependent functionally graded Kirchhoff and Mindlin plate models based on a modified couple stress theory.

It can be seen that, researches on the mechanical nonlinear behavior of microstructures have obtained great achievements. Therefore, this paper contributes a little to understanding the mechanical behavior of this structure.

2. Finite element formulations

Consider a homogeneous variable microplate with the length *a*, the width *b*, and the variable thickness *h* (x, y) as shown in Fig. 1.

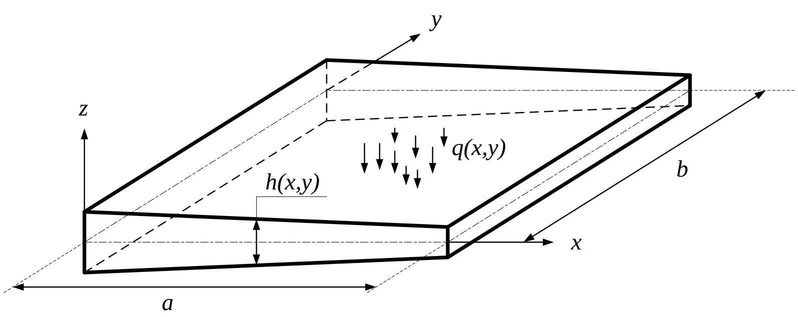

Fig. 1. The model of a microplate.

The displacement field of every point in the microplate is expressed as follows using Mindlin's first-order shear deformation theory [14]:

$$\begin{cases} u = u_o + z.\varphi_x \\ v = v_o + z.\varphi_y \\ w = w_o \end{cases} \tag{1}$$

in which $u, v,$ and w are the displacements along the *x*- *y*-, and *z*-directions, respectively; $u_o, v_o,$ and w_o are the displacements of the point in the neutral surface along the *x*- *y*-, and *z*-directions, respectively; φ_x and φ_y are the rotations of the cross-area around *y*- and *x*-axes, respectively.

According to the modified couple stress theory with only one material length scale parameter, the strain energy of the plate element is calculated as [16]:

$$U_e = \int_{V_e} \left(\sigma_{ij}\varepsilon_{ij} + m_{ij}.\chi_{ij} \right) dV_e \tag{2}$$

where summation on repeated indices is implied; σ_{ij} are the components of the stress tensor; ε_{ij} are the components of the strain tensor; m_{ij} are the components of the deviatoric part of the symmetric couple stress tensor; and χ_{ij} are the components of the symmetric curvature tensors, which are defined as:

$$\chi_{ij} = \frac{1}{2}\left(\frac{\partial \theta_i}{\partial x_j} + \frac{\partial \theta_j}{\partial x_i}\right), \quad i, j = x, y, z \tag{3}$$

and θ_i are the components of the rotation vector expressed as:

$$\begin{gathered}\theta_x = \frac{1}{2}\left(\frac{\partial w_0}{\partial y} - \varphi_y\right); \theta_y = \frac{1}{2}\left(-\frac{\partial w_0}{\partial x} + \varphi_x\right); \\ \theta_z = \frac{1}{2}\left(\frac{\partial v}{\partial x} - \frac{\partial u}{\partial y} + z.\frac{\partial \varphi_y}{\partial x} - z.\frac{\partial \varphi_x}{\partial y}\right).\end{gathered} \tag{4}$$

The bending strain is depended nonlinearly on the displacement field as follows [14]:

$$\begin{cases} \varepsilon_x = \dfrac{\partial u}{\partial x} + \dfrac{1}{2}\left(\dfrac{\partial \mathrm{w}}{\partial x}\right)^2 = \dfrac{\partial u_o}{\partial x} + \dfrac{1}{2}\left(\dfrac{\partial \mathrm{w}}{\partial x}\right)^2 + z.\dfrac{\partial \varphi_x}{\partial x} \\ \varepsilon_y = \dfrac{\partial v}{\partial y} + \dfrac{1}{2}\left(\dfrac{\partial \mathrm{w}}{\partial y}\right)^2 = \dfrac{\partial v_o}{\partial y} + \dfrac{1}{2}\left(\dfrac{\partial \mathrm{w}}{\partial y}\right)^2 + z.\dfrac{\partial \varphi_y}{\partial y} \\ \gamma_{xy} = \dfrac{\partial u}{\partial y} + \dfrac{\partial v}{\partial x} + \dfrac{\partial w}{\partial x}.\dfrac{\partial w}{\partial y} = \left(\dfrac{\partial u_o}{\partial y} + \dfrac{\partial v_o}{\partial x}\right) + \dfrac{\partial w}{\partial x}.\dfrac{\partial w}{\partial y} + z.\left(\dfrac{\partial \varphi_x}{\partial y} + \dfrac{\partial \varphi_y}{\partial x}\right) \end{cases} \tag{5}$$

Equation (5) is divided into the following components:

$$\{\varepsilon_L\} = \left\{\frac{\partial u_o}{\partial x}, \frac{\partial v_o}{\partial y}, \frac{\partial u_o}{\partial y} + \frac{\partial v_o}{\partial x}\right\}^T; \{\varepsilon_{NL}\} = \left\{\frac{1}{2}\left(\frac{\partial \mathrm{w}}{\partial x}\right)^2 \quad \frac{1}{2}\left(\frac{\partial \mathrm{w}}{\partial y}\right)^2 \quad \frac{\partial w}{\partial x}.\frac{\partial w}{\partial y}\right\}^T$$

$$\{\kappa\} = \left\{\frac{\partial \varphi_x}{\partial x}, \frac{\partial \varphi_y}{\partial y}, \frac{\partial \varphi_x}{\partial y} + \frac{\partial \varphi_y}{\partial x}\right\}^T$$

Therefore, the bending strain can be written as follows:

$$\{\varepsilon_b\} = \{\varepsilon_x, \varepsilon_y, \gamma_{xy}\}^T = \{\varepsilon_N\} + \{\varepsilon_{NL}\} + z.\{\kappa\} \tag{6}$$

The shear strain vector is defined in the following equation:

$$\{\varepsilon_s\} = \begin{Bmatrix} \gamma_{xz} \\ \gamma_{yz} \end{Bmatrix} = \begin{Bmatrix} \dfrac{\partial u}{\partial z} + \dfrac{\partial w}{\partial x} \\ \dfrac{\partial v}{\partial z} + \dfrac{\partial w}{\partial y} \end{Bmatrix} = \left\{\varphi_x + \frac{\partial w}{\partial x} \quad \varphi_y + \frac{\partial w}{\partial y}\right\}^T \tag{7}$$

The components of the symmetric curvature tentors are expressed as follows [14]:

$$\{\chi_b\} = \{\chi_x \quad \chi_y \quad \chi_z \quad \chi_{xy}\}^T; \{\chi_s\} = \{\chi_{yz} \quad \chi_{zx}\}^T \tag{8}$$

in which

$$\begin{aligned}
&\chi_x = \frac{1}{2}\left(\frac{\partial^2 w_0}{\partial y \partial x} - \frac{\partial \varphi_y}{\partial x}\right);\ \chi_y = -\frac{1}{2}\left(\frac{\partial^2 w_0}{\partial x \partial y} - \frac{\partial \varphi_x}{\partial y}\right);\\
&\chi_z = -\frac{1}{2}\left(-\frac{\partial \varphi_y}{\partial x} + \frac{\partial \varphi_x}{\partial y}\right);\ \chi_{xy} = \frac{1}{4}\left(\frac{\partial^2 w_0}{\partial y^2} - \frac{\partial \varphi_y}{\partial y}\right) - \frac{1}{4}\left(\frac{\partial^2 w_0}{\partial x^2} - \frac{\partial \varphi_x}{\partial x}\right);\\
&\chi_{yz} = -\frac{1}{4} z\left(-\frac{\partial^2 \varphi_y}{\partial x \partial y} + \frac{\partial^2 \varphi_x}{\partial y \partial y}\right) + \frac{1}{4}\left(\frac{\partial^2 v_0}{\partial x \partial y} - \frac{\partial^2 u_0}{\partial y \partial y}\right);\\
&\chi_{zx} = -\frac{1}{4} z\left(-\frac{\partial^2 \varphi_y}{\partial x \partial x} + \frac{\partial^2 \varphi_x}{\partial x \partial y}\right) + \frac{1}{4}\left(\frac{\partial^2 v_0}{\partial x \partial x} - \frac{\partial^2 u_0}{\partial x \partial y}\right).
\end{aligned} \tag{9}$$

Then, equation (8) can be expressed clearly as follows:

$$\{\chi_b\} = \frac{1}{4}\left\{\begin{matrix} 2\left(\frac{\partial^2 w_0}{\partial y \partial x} - \frac{\partial \varphi_y}{\partial x}\right) \\ -2\left(\frac{\partial^2 w_0}{\partial x \partial y} - \frac{\partial \varphi_x}{\partial y}\right) \\ -2\left(-\frac{\partial \varphi_y}{\partial x} + \frac{\partial \varphi_x}{\partial y}\right) \\ \left(\frac{\partial^2 w_0}{\partial y^2} - \frac{\partial \varphi_y}{\partial y}\right) - \left(\frac{\partial^2 w_0}{\partial x^2} - \frac{\partial \varphi_x}{\partial x}\right) \end{matrix}\right\}; \{\chi\}_s = \{\chi_{sm}\} + z.\{\chi_{ss}\} \tag{10}$$

where $\{\chi_{sm}\} = \frac{1}{4}\left\{\begin{matrix} \left(\frac{\partial^2 v_0}{\partial x \partial y} - \frac{\partial^2 u_0}{\partial y \partial y}\right) \\ \left(\frac{\partial^2 v_0}{\partial x \partial x} - \frac{\partial^2 u_0}{\partial x \partial y}\right) \end{matrix}\right\}; \{\chi_{ss}\} = \frac{1}{4}\left\{\begin{matrix} \frac{\partial^2 \varphi_y}{\partial x \partial y} - \frac{\partial^2 \varphi_x}{\partial y \partial y} \\ \frac{\partial^2 \varphi_y}{\partial x \partial x} - \frac{\partial^2 \varphi_x}{\partial y \partial x} \end{matrix}\right\}$

Now, the stress fields are calculated as follows:

- *The normal stress field:*

$$\{\sigma_b\} = \left\{\begin{matrix} \sigma_x \\ \sigma_y \\ \tau_{xy} \end{matrix}\right\} = [D_b].\left\{\begin{matrix} \varepsilon_x \\ \varepsilon_y \\ \gamma_{xy} \end{matrix}\right\} = [D_b]\{\varepsilon_N\} + [D_b]\{\varepsilon_{NL}\} + z.[D_b].\{\kappa\} \tag{11}$$

in which

$$\left[D_b\right]=\frac{E}{1-\mu^2}\begin{bmatrix}1 & \mu & 0\\ \mu & 1 & 0\\ 0 & 0 & \dfrac{1-\mu}{2}\end{bmatrix}$$ is the constant material matrix;

E and μ are the Young's modulus and Poisson's ration, respectively.

- *The shear stress field:*

$$\{\tau\}=\left[D_s\right]\{\varepsilon_s\} \tag{12}$$

in which $\left[D_s\right]=\begin{bmatrix}G & 0\\ 0 & G\end{bmatrix};G=\dfrac{E}{2(1+\mu)}$.

- *The components of the deviatoric part of the symmetric couple stress tensor* [14]:

$$\{m\}=\left[D_o\right]\{\chi_b\};\{n\}=\left[D_{os}\right]\{\chi_s\} \tag{13}$$

where

$\left[D_0\right]=\dfrac{E.l_o^2}{1+\mu}\begin{bmatrix}1 & 0 & 0 & 0\\ 0 & 1 & 0 & 0\\ 0 & 0 & 1 & 0\\ 0 & 0 & 0 & 1\end{bmatrix}$ and $\left[D_{\mathrm{os}}\right]=\dfrac{E.l_o^2}{2(1+\mu)}\begin{bmatrix}1 & 0\\ 0 & 1\end{bmatrix}$ are the constant material matrices;

l_o is the length-scale parameter, which depends on materials.

Then, the strain energy is now expressed as:

$$U_e=\frac{1}{2}\int_{S_e}\begin{pmatrix}\{\varepsilon_N\}^T.[A].\{\varepsilon_N\}+\{\varepsilon_{NL}\}^T.[A].\{\varepsilon_{NL}\}+\{\kappa\}^T.[B].\{\kappa\}\\ +\{\varepsilon_s\}^T[A].\{\varepsilon_s\}+\{\chi_b\}^T.[C].\{\chi_b\}+\{\chi_b\}^T.[H].\{\chi_b\}\\ +\{\chi_{sb}\}^T.[Y].\{\chi_{sb}\}+\{\chi_{ss}\}^T.[X].\{\chi_{ss}\}\end{pmatrix}dxdy \tag{14}$$

where

$$\begin{aligned}&\left([A],[B],[D]\right)=\int_{-\frac{h}{2}}^{\frac{h}{2}}\left(1,z,z^2\right)dz.\left[D_b\right];[A]=\frac{5}{6}\int_{-\frac{h}{2}}^{\frac{h}{2}}dz.\left[D_s\right]\\ &\left([C],[H]\right)=\int_{-\frac{h}{2}}^{\frac{h}{2}}(1,z)\,dz.\left[D_o\right];\left([Y],[X]\right)=\int_{-\frac{h}{2}}^{\frac{h}{2}}(1,z)\,dz.\left[D_{os}\right]\end{aligned} \tag{15}$$

A four-node quadrilateral element is utilized in this paper, with each node having five degrees of freedom:

$$\{q_e\} = \{\{q_1\} \quad \{q_2\} \quad \{q_3\} \quad \{q_4\}\}^T ; \{q_i\} = \{u_{0i} \quad v_{0i} \quad w_{0i} \quad \varphi_{xi} \quad \varphi_{yi}\}^T$$

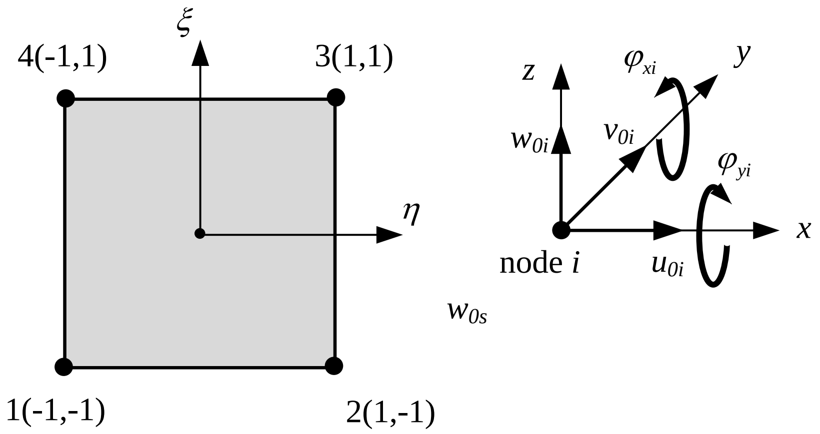

Fig. 2. A four-node quadrilateral element.

Then, the components of the strain tensor and the components of the symmetric curvature tensors are expanded by the Lagrange shape functions and the element displacement vector as follows:

$$\begin{aligned}&\{\varepsilon_N\} = [B_1^L]\{q_e\}; \{\varepsilon_{NL}\} = [B_1^{NL}]\{q_e\}; \{\kappa\} = [B_2]\{q_e\}; \{\varepsilon_s\} = [B_3]\{q_e\};\\ &\{\chi_b\} = [B_4]\{q_e\}; \{\chi_{sm}\} = [B_5]\{q_e\}; \{\chi_{ss}\} = [B_6]\{q_e\}.\end{aligned} \tag{16}$$

in which

$$B_1^L = \sum_{i=1}^{4}\begin{bmatrix} \frac{\partial N_i}{\partial x} & 0 & 0 & 0 & 0 \\ 0 & \frac{\partial N_i}{\partial y} & 0 & 0 & 0 \\ \frac{\partial N_i}{\partial y} & \frac{\partial N_i}{\partial x} & 0 & 0 & 0 \end{bmatrix}; [B_1^{NL}] = \frac{1}{2}\begin{bmatrix} \frac{\partial w}{\partial x} & 0 \\ 0 & \frac{\partial w}{\partial y} \\ \frac{\partial w}{\partial y} & \frac{\partial w}{\partial x} \end{bmatrix}\sum_{i=1}^{4}\begin{bmatrix} 0 & 0 & \frac{\partial N_i}{\partial x} & 0 & 0 \\ 0 & 0 & \frac{\partial N_i}{\partial y} & 0 & 0 \end{bmatrix}$$

$$[B_2] = \sum_{i=1}^{4}\begin{bmatrix} 0 & 0 & 0 & \frac{\partial N_i}{\partial x} & 0 \\ 0 & 0 & 0 & 0 & \frac{\partial N_i}{\partial y} \\ 0 & 0 & 0 & \frac{\partial N_i}{\partial y} & \frac{\partial N_i}{\partial x} \end{bmatrix}; [B_3] = \sum_{i=1}^{4}\begin{bmatrix} 0 & 0 & \frac{\partial N_i}{\partial x} & 1 & 0 \\ 0 & 0 & \frac{\partial N_i}{\partial y} & 0 & 1 \end{bmatrix}$$

$$
\left[B_4\right]=\frac{1}{4}\sum_{i=1}^{4}\begin{bmatrix} 0 & 0 & 2\dfrac{\partial^2 N_i}{\partial y\partial x} & 0 & -2\dfrac{\partial N_i}{\partial x} \\ 0 & 0 & -2\dfrac{\partial^2 N_i}{\partial x\partial y} & 2\dfrac{\partial N_i}{\partial y} & 0 \\ 0 & 0 & 0 & -2\dfrac{\partial N_i}{\partial y} & 2\dfrac{\partial N_i}{\partial x} \\ 0 & 0 & \dfrac{\partial^2 N_i}{\partial y^2}-\dfrac{\partial^2 N_i}{\partial x^2} & \dfrac{\partial N_i}{\partial x} & -\dfrac{\partial N_i}{\partial y} \end{bmatrix}
$$

$$
\left[B_5\right]=\sum_{i=1}^{4}\frac{1}{4}\begin{bmatrix} -\dfrac{\partial^2 N_i}{\partial y\partial y} & \dfrac{\partial^2 N_i}{\partial x\partial y} & 0 & 0 & 0 \\ -\dfrac{\partial^2 N_i}{\partial x\partial y} & \dfrac{\partial^2 N_i}{\partial x\partial x} & 0 & 0 & 0 \end{bmatrix};\left[B_6\right]=\sum_{i=1}^{4}\frac{1}{4}\begin{bmatrix} 0 & 0 & 0 & -\dfrac{\partial^2 N_i}{\partial y\partial y} & \dfrac{\partial^2 N_i}{\partial x\partial y} \\ 0 & 0 & 0 & -\dfrac{\partial^2 N_i}{\partial y\partial x} & \dfrac{\partial^2 N_i}{\partial x\partial x} \end{bmatrix}
$$

Substituting into equation (14), one gets:

$$
U_e=\frac{1}{2}.\{q_e\}^T.\left[\int_{S_e}\begin{pmatrix} \left[B_1^N\right]^T.[A].\left[B_1^L\right]+\left[B_1^{NL}\right]^T.[A].\left[B_1^{NL}\right] \\ +\left[B_2\right]^T.[B].\left[B_2\right]+\left[B_3\right]^T.[A].\left[B_3\right] \\ +\left[B_4\right]^T.[C].\left[B_4\right]+\left[B_5\right]^T.[H].\left[B_5\right] \\ +\left[B_6\right]^T.[X].\left[B_6\right] \end{pmatrix}dxdy\right].\{q_e\} \tag{17}
$$

Therefore, the element stiffness matrix of the microplate element is obtained as:

$$
\left[K_e\right]=\left[K_e^L\right]+\left[K_e^{NL}\right] \tag{18}
$$

where the linear and nonlinear element stiffness matrices are expressed as follows:

$$
\left[K_e^L\right]=\int_{S_e}\begin{pmatrix} \left[B_1^N\right]^T.[A].\left[B_1^L\right]+\left[B_2\right]^T.[B].\left[B_2\right]+\left[B_3\right]^T.[A].\left[B_3\right] \\ +\left[B_4\right]^T.[C].\left[B_4\right]+\left[B_5\right]^T.[H].\left[B_5\right]+\left[B_6\right]^T.[X].\left[B_6\right] \end{pmatrix}dxdy
$$

$$
\left[K_e^{NL}\right]=\int_{S_e}\left(\left[B_1^{NL}\right]^T.[A].\left[B_1^{NL}\right]\right)dxdy
$$

The work done by the external forces is calculated as:

$$
A_e=\int_{S_e}\{u\}^T\{f\}dS_e \tag{19}
$$

where

$$\{u\}^T = \{u_0 \quad v_0 \quad w_0 \quad \varphi_x \quad \varphi_y\} = \{q_e\}^T.[N]^T; \{f\} = \{0 \quad 0 \quad q(x,y) \quad 0 \quad 0\}^T$$

Equation (19) becomes:

$$A_e = \{q_e\}^T \int_{S_e} [N]^T \{f\} dx\mathrm{d}y \tag{20}$$

Thus, one gets:

$$F_e = \int_{S_e} \left([N]^T \{f\}\right) dx\mathrm{d}y \tag{21}$$

The static equilibrium equation for the entire microplate is derived after assembling the components of element matrices and vectors:

$$\left(\left[K^L\right] + \left[K^{NL}\right]\right)\{Q\} = \{F\} \tag{22}$$

To solve equation (22), the Newton-Rapshon method is used.

3. Numerical results and discussions

3.1. Verification example

This section carries out a verification example to confirm the present theory and mechanical model. Consider a fully simply supported square homogeneous microplate with dimensions and material properties [16]: h = 17.6·10^{-6} m (h is unchanged), a = b = 20h, l_0 = 0.2h, Young's modulus E = 1.44 GPa, Poisson's ratio $\mu = 0.38$. The sinusoidally distributed load is applied as follows:

$$q(x,y) = q_o \sin\left(\frac{\pi}{2}x\right)\sin\left(\frac{\pi}{2}y\right) \tag{23}$$

in which q_o can be found in the normalized force as follows:

$$q^* = \frac{q_o a^4}{Eh^4} \tag{24}$$

The non-dimensional maximum deflection is defined as:

$$w^* = \frac{100Eh^3}{q_o a^4} w\left(\frac{a}{2}, \frac{a}{2}\right) \tag{25}$$

The following Fig. 3 presents the comparative non-dimensional maximum deflections between this work and Thai et al. [16]:

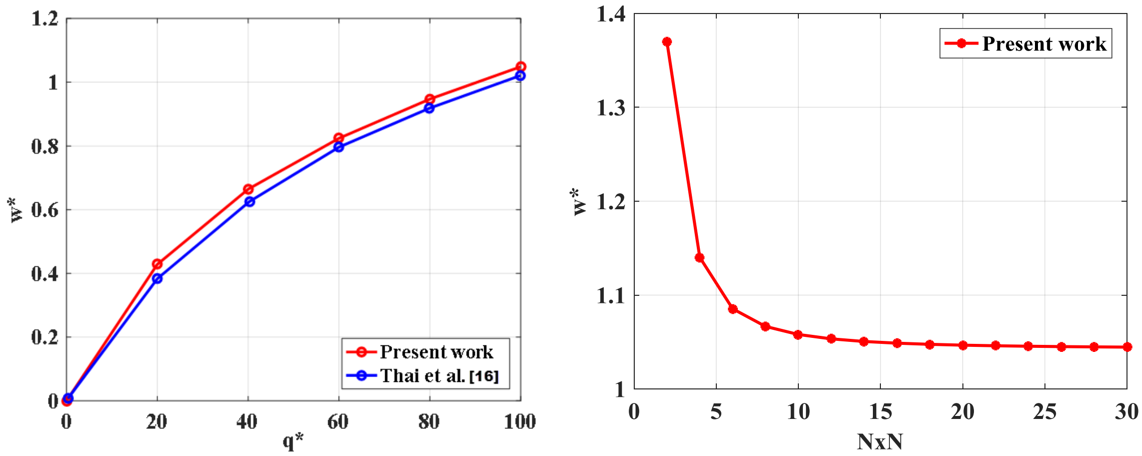

a) *b)*

Fig. 3. a) Comparative non-dimensional maximum deflections;
b) The convergence of the nondimensional maximum deflection.

It can be seen that, the numerical results of this work meet a good agreement with those of Thai et al. [16]. Fig. 3 also shows that for the 16×16 mesh size, the result reaches a convergent value.

3.2. Parameter study

3.2.1. Effects of variable thickness

Firstly, the effects of variable thickness on the static bending of microplates are investigated. Consider a fully simply supported square homogeneous microplate with dimensions and material properties as shown in the verification example above. The sinusoidally distributed load is applied as shown in equations (20) and (21), herein $q^* = 100$. Let h_o = 17.6.10^{-6} m be the base thickness of the plate, four cases of variable thickness are considered.

- Case 1: Unchanged; $h_c(x,y) = h_o$.

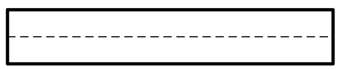

- Case 2: Linear variable thickness in the *x*-direction; $h_c(x,y) = h_o\left(-\dfrac{x}{2a} + 1\right)$.

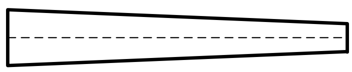

- Case 3: Linear variable thickness in both the *x*- and *y*-directions; $h(x,y) = h_o\left(-\dfrac{2x}{3a} - \dfrac{2y}{15b} + 15\right)$.

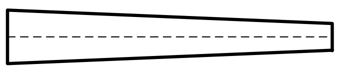

- Case 4: Parabolic variable thickness in the x-direction; $h(x,y) = h_o\left(-\dfrac{x^2}{2a^2}+1\right)$.

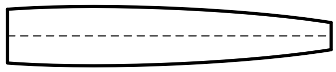

The non-dimentional deflection responses of microplates are presented in the following Fig. 4.

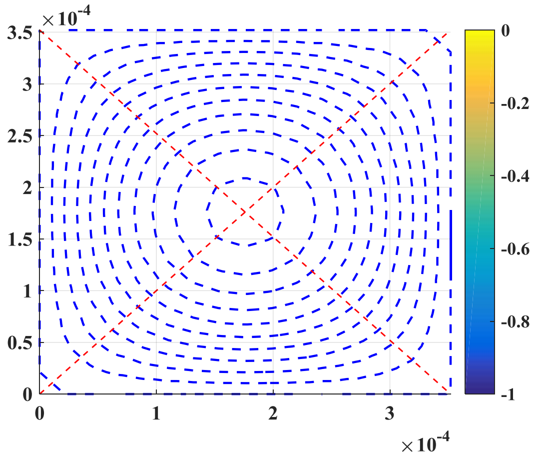

a) Case 1

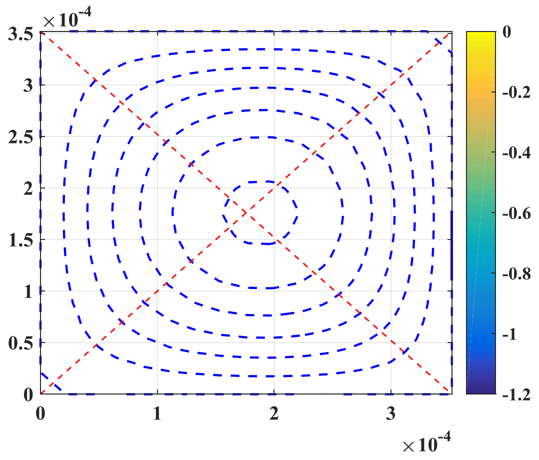

b) Case 2

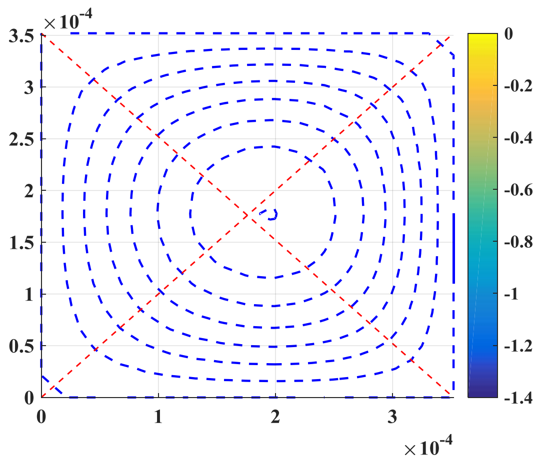

c) Case 3

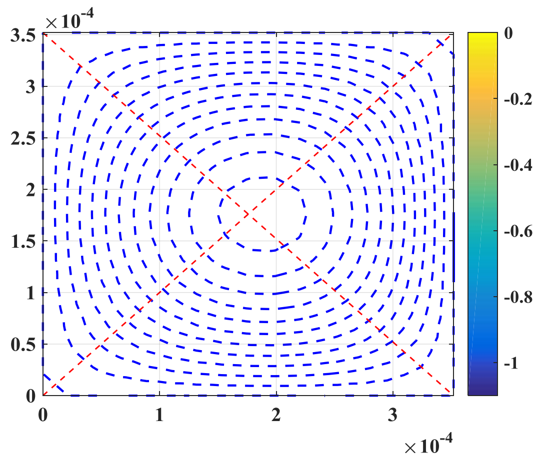

d) Case 4

Fig. 4. The dependence of non-dimentional deflection response (w/h_0)
of the microplate on the variable thickness.

3.2.2. Effects of lengh-scale parameter

Next, the effects of lengh-scale parameter on the static respone of microplates are examined. The microplate (case 1) in the previous subsection is considered again.

Let the lengh-scale parameter l_o change in a range from 0 to 1. The nondimensional deflection of microplate is presented in Fig. 5 bellow.

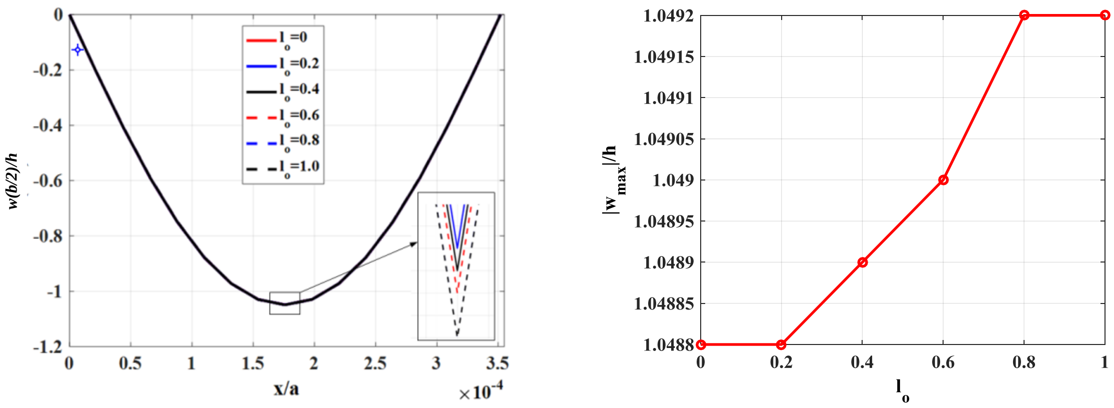

Fig. 5. Effects of length-scale parameter.

The beam deflection rises as the length-scale parameter l_o grows, as seen in Fig. 5.

3.2.3. Effect of external load

Finally, the effects of external load on the static bending behavior of microplates are explored (Fig. 6). Consider a fully simply supported microplate as shown in the first subsection. Herein, non-dimensional external load q^* gets the values from 0 to 100.

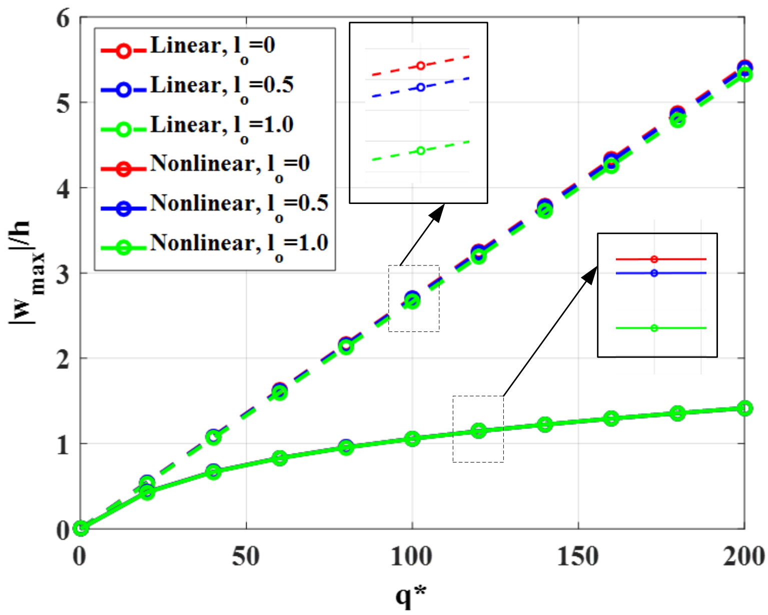

Fig. 6. Effect of external load.

4. Conclusions

This paper presents the nonlinear static bending analysis of variable thickness microplates by using the finite element method and modified couple stress. The present theory and mathematical model are confirmed by comparing the numerical data with those of open literatues. Some novel findings can be summed up as follows:

- The variation of the plate thickness has a significant influence on the static response of the microplate. A plate with a symmetrical structure and a symmetrical constainst has a symmetrical deformation. In the case of plates with variable thickness, the position of the point with the largest deflection tends to shift to the position where the plate has a small thickness.

- The length-scale parameter also affects the mechanical response of the plate. As l_o increases, beam deflection decreases. The reason is that the stiffness of the plate decreases as l_o increases.

- The applied external load has a great influence on the static response of the plate. the value of the load increases, the deflection of the plate increases. When the load is small, there is no big difference between the displacements in the linear and nonlinear cases. However, as the load increases, this difference increases greatly.

The computed data can be used as a good reference in the use and design of these types of structures in engineering practice.

References

[1] M. P. Singh, "Application of Biolog FF MicroPlate for substrate utilization and metabolite profiling of closely related fungi," *J. Microbiol. Methods*, vol. 77, no. 1, pp. 102-108, 2009, doi: https://doi.org/10.1016/j.mimet.2009.01.014.

[2] M.-B. A. Ashour, S. J. Gee, and B. D. Hammock, "Use of a 96-well microplate reader for measuring routine enzyme activities," *Anal. Biochem.*, vol. 166, no. 2, pp. 353-360, 1987, doi: https://doi.org/10.1016/0003-2697(87)90585-9.

[3] F. V Plapp and J. M. Rachel, "Automation in blood banking. Machines for clumping, sticking, and gelling," *Am. J. Clin. Pathol.*, vol. 98, no. 4 Suppl. 1, p. S17-21, 1992, [Online]. Available: http://europepmc.org/abstract/MED/1344699.

[4] S.-B. Huang *et al.*, "Development of a pneumatically driven active cover lid for multi-well microplates for use in perfusion three-dimensional cell culture," *Sci. Rep.*, vol. 5, no. 1, p. 18352, 2015, doi: 10.1038/srep18352.

[5] A. Gholipour, H. Farokhi, and M. H. Ghayesh, "In-plane and out-of-plane nonlinear size-dependent dynamics of microplates," *Nonlinear Dyn.*, vol. 79, no. 3, pp. 1771-1785, 2015, doi: 10.1007/s11071-014-1773-7.

[6] C.-L. Thanh, L. V Tran, T. Q. Bui, H. X. Nguyen, and M. Abdel-Wahab, "Isogeometric analysis for size-dependent nonlinear thermal stability of porous FG microplates," *Compos. Struct.*, vol. 221, p. 110838, 2019, doi: https://doi.org/10.1016/j.compstruct.2019.04.010.

[7] L.-L. Ke, Y.-S. Wang, J. Yang, and S. Kitipornchai, "Free vibration of size-dependent Mindlin microplates based on the modified couple stress theory," *J. Sound Vib.*, vol. 331, no. 1, pp. 94-106, 2012, doi: https://doi.org/10.1016/j.jsv.2011.08.020.

[8] Nguyen Dinh Duc, Seung-Eock Kim, Vu Thi ThuyAnh, Vu Minh Anh, "Vibration and nonlinear dynamic analysis of variable thickness sandwich laminated composite panel in thermal environment," *Journal Sandwich Structures and Materials*, 23(5), pp. 1541-1570, 2021.

[9] Phuc Pham Minh, Thom Van Do, Doan Hong Duc, Nguyen Dinh Duc, "The stability of cracked rectangular plate with variable thickness using phase field method," Thin Walled Structures, Vol. 129, pp. 157-165, 2018.

[10] S.-X. Chen, S. Sahmani, and B. Safaei, "Size-dependent nonlinear bending behavior of porous FGM quasi-3D microplates with a central cutout based on nonlocal strain gradient isogeometric finite element modelling," *Eng. Comput.*, vol. 37, no. 2, pp. 1657-1678, 2021, doi: 10.1007/s00366-021-01303-z.

[11] F. Alinaghizadeh and M. Shariati, "Nonlinear analysis of size-dependent annular sector and rectangular microplates under transverse loading and resting on foundations based on the modified couple stress theory," *Thin-Walled Struct.*, vol. 149, p. 106583, 2020, doi: https://doi.org/10.1016/j.tws.2019.106583.

[12] M. H. Ghayesh, H. Farokhi, A. Gholipour, and M. Tavallaeinejad, "Nonlinear oscillations of functionally graded microplates," *Int. J. Eng. Sci.*, vol. 122, pp. 56-72, 2018, doi: https://doi.org/10.1016/j.ijengsci.2017.03.014.

[13] A. R. Askari and M. Tahani, "Size-dependent dynamic pull-in analysis of geometric non-linear micro-plates based on the modified couple stress theory," *Phys. E Low-dimensional Syst. Nanostructures*, vol. 86, pp. 262-274, 2017, doi: https://doi.org/10.1016/j.physe.2016.10.035.

[14] M. Şimşek, M. Aydın, H. H. Yurtcu, and J. N. Reddy, "Size-dependent vibration of a microplate under the action of a moving load based on the modified couple stress theory," *Acta Mech.*, vol. 226, no. 11, pp. 3807-3822, 2015, doi: 10.1007/s00707-015-1437-9.

[15] H. Farokhi, M. H. Ghayesh, A. Gholipour, and M. Tavallaeinejad, "Nonlinear oscillations of viscoelastic microplates," *Int. J. Eng. Sci.*, vol. 118, pp. 56-69, 2017, doi: https://doi.org/10.1016/j.ijengsci.2017.05.006.

[16] H.-T. Thai and D.-H. Choi, "Size-dependent functionally graded Kirchhoff and Mindlin plate models based on a modified couple stress theory," *Compos. Struct.*, vol. 95, pp. 142-153, 2013, doi: https://doi.org/10.1016/j.compstruct.2012.08.023.

PHÂN TÍCH PHI TUYẾN UỐN TĨNH CỦA TẤM MICRO CÓ CHIỀU DÀY THAY ĐỔI SỬ DỤNG PHƯƠNG PHÁP PHẦN TỬ HỮU HẠN VÀ LÝ THUYẾT CẶP ỨNG SUẤT CẢI TIẾN

Nguyễn Thị Cẩm Nhung, Lê Minh Hoàng, Trần Văn Kế,
Nguyễn Thị Dung, Phùng Văn Minh

Tóm tắt: *Bài báo trình bày phân tích phi tuyến uốn tĩnh của tấm micro có chiều dày thay đổi sử dụng lý thuyết phần tử hữu hạn và cặp ứng suất cải tiến. Lý thuyết và mô hình toán học được khẳng định bằng cách so sánh kết quả số với các tài liệu chính xác đã được công bố. Nghiên cứu tham số được tiến hành để đánh giá các đặc tính cơ học của kết cấu, đặc biệt là ảnh hưởng của tính phi tuyến. Kết quả tính toán của bài báo có thể được tham khảo khi tính toán, thiết kế các dạng kết cấu kích cỡ micro trong thực tế kỹ thuật.*

Từ khóa: Phi tuyến; tấm kích thước micro; lý thuyết cặp ứng suất cải tiến; uốn tĩnh; chiều dày thay đổi.

Received: 05/01/2022; *Revised:* 09/05/2022; *Accepted for publication:* 02/06/2022

❑